TWO-DIMENSIONAL PARA-, ORTHO-, AND BI-MAGNETOEXCITONS INTERACTING WITH QUANTUM POINT VORTICES

S. A. Moskalenko[1], V. A. Moskalenko[1], P. I. Khadzhi[1], I. V. Podlesny[1], M. A. Liberman[2], and I. A. Zubac[1]

[1]*Institute of Applied Physics, Academy of Sciences of Moldova, Academiei str. 5, Chisinau, MD-2028 Republic of Moldova*
[2]*Nordic Institute for Theoretical Physics (NORDITA) KTH and Stockholm University, Roslagstullsbacken 23, Stockholm, SE-106 91 Sweden*
E-mail: exciton@phys.asm.md

Abstract

The theory of two-dimensional (2D) magnetoexcitons was enlarged taking into account the electron–hole (e–h) exchange Coulomb interaction, which appears when the conduction and valence electrons belong partially to both bands. This Coulomb exchange interaction leads to the linear dispersion law of para-magnetoexcitons. Spectral properties and the new luminescence band, which arise owing to the existence of the metastable bound state, are discussed. The thermodynamic properties and the Bose–Einstein condensation conditions for para- and ortho-magnetoexcitons are described. Taking into account the vector potential of the Chern–Simons gauge field the anisotropy of the 2D magnetoexciton magnetic mass was revealed.

1. Introduction

The properties of 2D magnetoexcitons are as follows. The Lorentz force determines the Landau quantization (LQ) of electrons and holes separately. Their LQ states are determined by the cyclotron energies, the radii of the orbits, and the gyration points around which the oscillations take place. The gyration points depend on the wave vectors of the particles. The cyclotron energies depend on the particle effective masses, whereas the radii of the orbits are determined by the magnetic length and do not depend on the effective masses at all. This property is referred to as the hidden symmetry [1].

The structure of the magnetoexciton is shown in Fig. 1. It looks as an electric dipole with arm $\vec{d} = \left[\vec{k} \times \vec{z}\right] l_0^2$ oriented perpendicular to the center-of-mass wave vector $\vec{k}$ and with length $d = kl_0^2$, where l_0 is the magnetic length.

If wave vector $\vec{k}$ is zero, then two electron clouds are overposed and, because of the equal radii of the orbits, these magnetoexcitons with $\vec{k} = 0$ look as completely neutral compound particles. The magnetoexcitons with wave vectors $\vec{k} = 0$ form an ideal Bose gas [2].

The molecule formation from these two magnetoexcitons will now be discussed. Two magnetoexcitons being confined on the 2D layer on the finite limited size determined by the wave function of their relative motion can form the bound states of the molecular type, as shown in Fig. 2. The distance between two magnetoexcitons in the frame of the bound state and their wave vectors are interdependent due to the Heisenberg uncertainty relation. It means that these dipoles have changing arms, which cannot be considered either rigid or constant. More so, the smaller the dipole arm, the greater the distance between them.

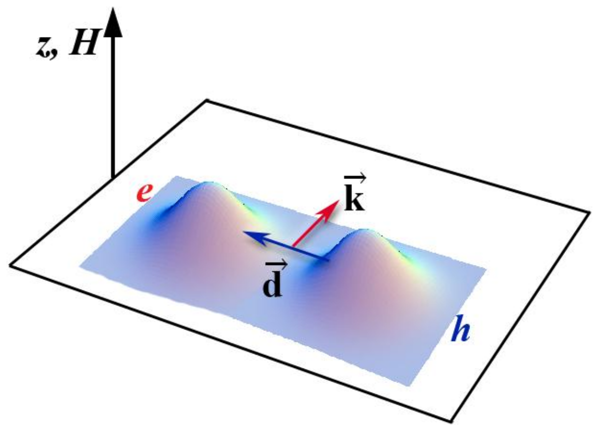

Fig. 1. Electric dipole model of the magnetoexciton with $\vec{k} \neq 0$.

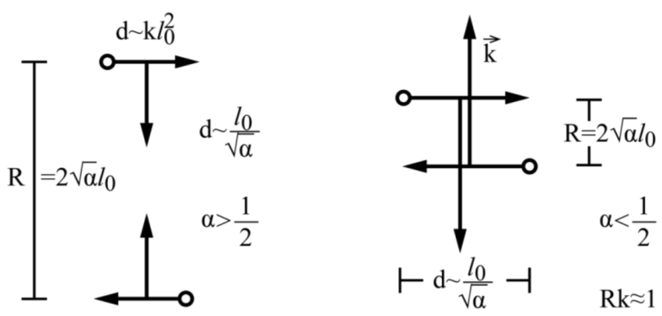

Fig. 2. Bound state of two magnetoexcitons with variational wave functions
$\varphi_2(k) \sim (kl_0)^2 e^{-\alpha(kl_0)^2}$.

It is significant that we deal with the molecule in the rest with a wave vector of $\vec{k} = 0$. It means that, in our case, the electric dipoles have wave vectors with opposite directions and antiparallel dipole moments. Because of the full neutrality of the magnetoexcitons with $\vec{k} = 0$, the wave function of the relative motion should have the maximum outside the point $\vec{k} = 0$; that is, in the momentum space representation, it should be on the ring, as shown in Fig. 3.

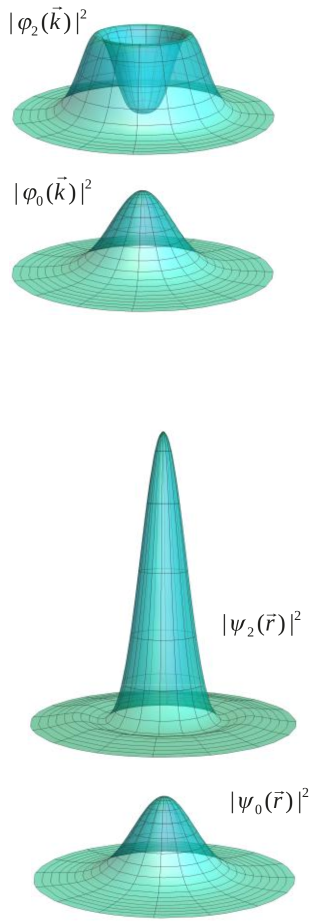

Fig. 3. Variational wave functions $\varphi_n(k)$ describing the bound states (a) in momentum representation $\varphi_0(k) \sim e^{-\alpha(kl_0)^2}$, $\varphi_2(k) \sim (kl_0)^2 e^{-\alpha(kl_0)^2}$ and (b) in real space representation $\psi_0(r) \sim \exp[-r^2/(4\alpha l_0^2)]$, $\psi_2(r) \sim \left(1 - r^2/(4\alpha l_0^2)\right)\exp[-r^2/(4\alpha l_0^2)]$.

The functions have variational parameter α, which will minimize the Coulomb interaction of the particles involved in the molecule formation. The spin structure of four particles, namely, two electrons and two holes, can be chosen in four ways. The most interesting case was the combination of the spin of two electrons in singlet or triplet forms. In addition, the spin structures of two holes were organized in singlet or triplet forms. The spin structures of four particles can be of the triplet–triplet or singlet–singlet types. The mixed versions are forbidden due to the hidden symmetry. As one can see from Fig. 4, other possibilities are due to the correlations of the spins of the electron and the hole in the frame of each exciton, what gives rise to ortho and para spin states.

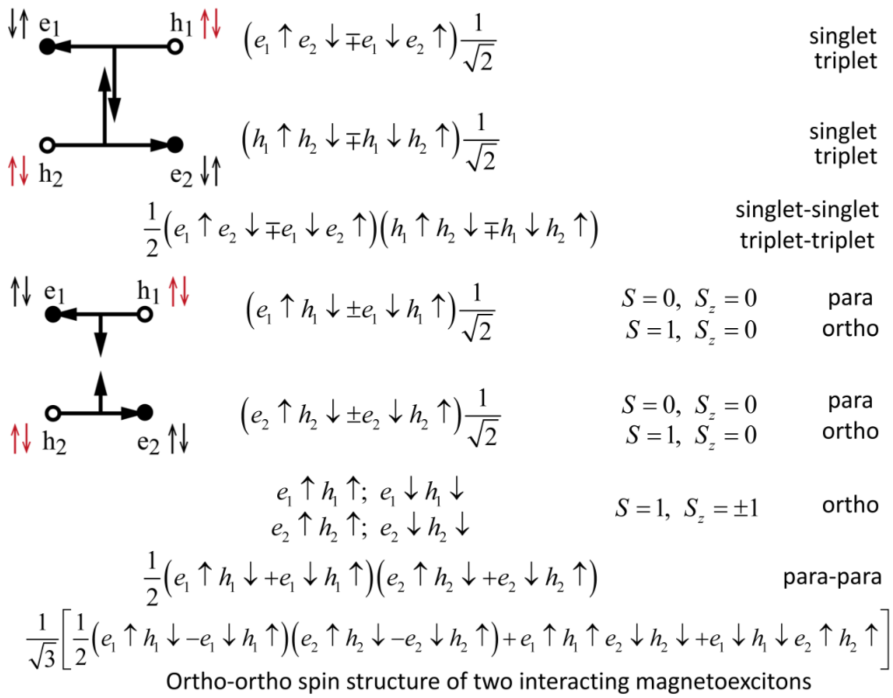

Fig. 4. Spin structure of two magnetoexcitons.

Four different spin structures were studied, and the Coulomb interaction integrals were calculated. The encountered Feynman diagrams containing the solid electron lines and the dashed hole lines can have an odd number of intersections, or an even number of intersections, or none intersections. All of them (Fig. 5) can be grouped in two main terms with spins structure parameter η, which takes four different values, namely, $+1,\ -1,\ +1/2,\ -1/2$:

$$E_{Bimex} = \frac{\langle \psi_{Bimex}(0,\eta) | H_{Coul}^{LLL} | \psi_{Bimex}(0,\eta) \rangle}{\langle \psi_{Bimex}(0,\eta) | \psi_{Bimex}(0,\eta) \rangle};$$

$$\langle \psi_{Bimex}(0,\eta) | H_{Coul}^{LLL} | \psi_{Bimex}(0,\eta) \rangle = \left\langle \begin{array}{l} \text{Feynman diagrams} \\ \text{without intersections or} \\ \text{with even numbers} \\ \text{of intersections} \end{array} \right\rangle + \eta \left\langle \begin{array}{l} \text{Feynman diagrams with} \\ \text{odd numbers} \\ \text{of intersections} \end{array} \right\rangle;$$

$$\langle \psi_{Bimex}(0,\eta) | \psi_{Bimex}(0,\eta) \rangle = 2\left(1-\eta L_n(\alpha)\right), \text{ where}$$

$\eta = 1$ triplet–triplet spin structures of 2e+2h,

$\eta = -1$ singlet–singlet spin structures of 2e+2h,

$\eta = \frac{1}{2}$ ortho–ortho magnetoexcitons,

$\eta = -\frac{1}{2}$ para–para magnetoexcitons. (1)

The exact analytical calculations were performed because the binding energy was expected to be small or absent at all.

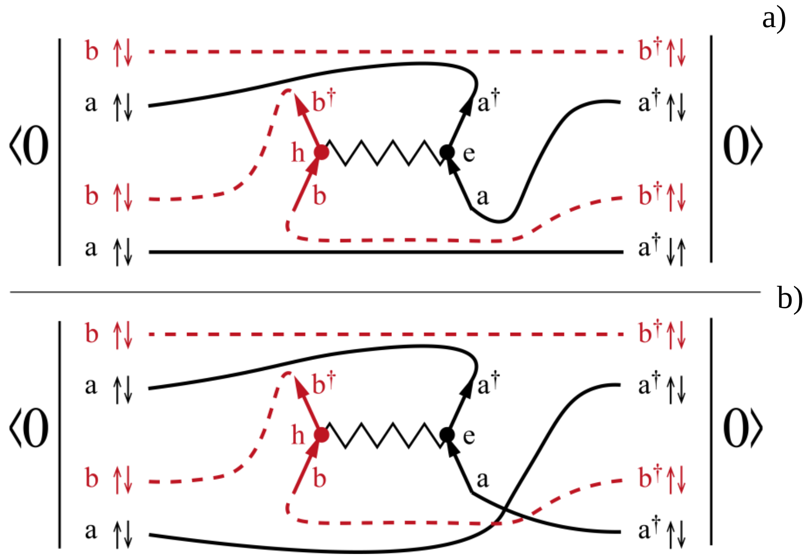

Fig. 5. Feynman diagrams describing the Coulomb electron–hole (e–h) interactions in the frame of the metastable bound state of two magnetoexcitons: (a) the case without intersections and (b) the case with one intersection.

The determined total energy of the Coulomb interaction as a function of variational parameter α is shown in Fig. 6.

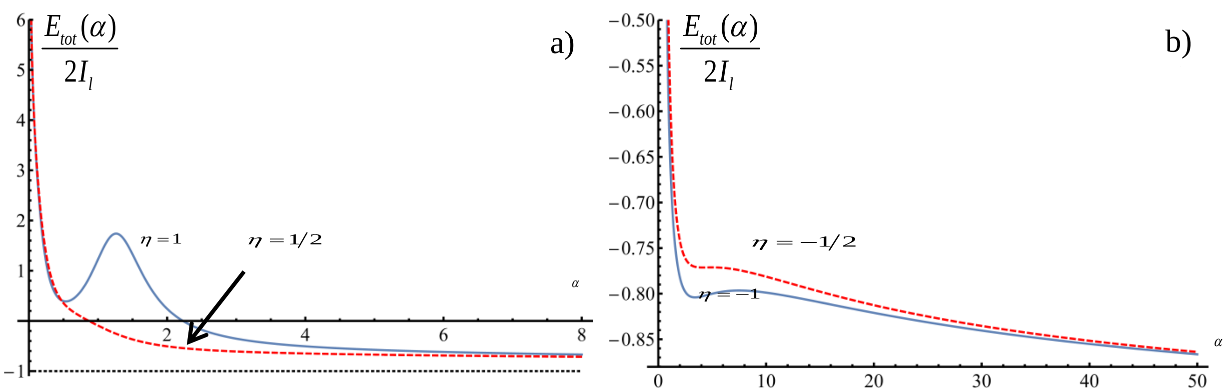

Fig. 6. Total energies of two bound 2D magnetoexcitons with wave vectors $\vec{k}$ and $-\vec{k}$, with different spin structures $\eta = \pm 1, \pm 1/2$ and with the variational wave function $\varphi_2(k)$ as a function of parameter α: (a) the case $\eta = 1,\ 1/2$ and (b) the case $\eta = -1, -1/2$. The total energies are normalized to the value $2I_l$, where I_l is the ionization potential of a free magnetoexciton with wave vector $\vec{k} = 0$.

The energy of two free magnetoexcitons with $k = 0$ is represented by the -1 line. At any α value, stable bound states are absent. All the states are unstable as regards the dissociation in two free magnetoexcitons with $k = 0$. However, despite this fact, in the triplet–triplet spin configuration, a metastable bound state with a considerable energy barrier of the order of two ionization potentials of two free magnetoexcitons was revealed. If we used the dipole–dipole interaction, we could not meet with the metastable bound state. Two antiparallel 2D dipole moments repeal each other, and their interaction energy is positive, whereas two parallel 2D dipoles attract each other. It is evident from the formulas below:

$$V_{\vec{d}_1\vec{d}_2} = \frac{e^2}{\varepsilon_0}\left[\frac{\vec{d}_1\cdot\vec{d}_2}{R^3} - \frac{3(\vec{d}_1\cdot\vec{R})(\vec{d}_2\cdot\vec{R})}{R^5}\right];$$

$$V_{\substack{(\uparrow\uparrow)\\(\uparrow\downarrow)}}(R) = \pm\frac{e^2d^2}{\varepsilon_0 R^3}\left(1-3\cos^2\varphi\right) \simeq \mp\frac{e^2d^2}{2R^3\varepsilon_0}; \qquad \overline{\cos^2\varphi} = \frac{1}{2}. \tag{2}$$

Despite these properties of the dipole–dipole interaction, which can give only a rough picture of the Coulomb interaction in the frame of confined particles, the metastable bound state can exist.

2. Tunneling and the New Luminescence Band

The tunneling properties and the new luminescence band arising due to the existence of the metastable bound state will now be discussed using Fig. 7, where an effective rectangular barrier with height *U–E* and with length l_b was introduced.

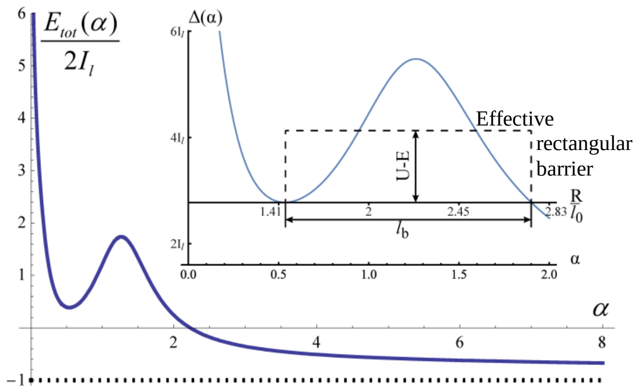

Fig. 7. Tunneling property of the metastable bound state.

The coefficient of the transparency of the energy barrier was estimated as 4%:

$$T = e^{-\frac{2}{\hbar}\sqrt{2M(U-E)}l_b} \sim e^{-3.2} \sim 10^{-1.4} \approx 0.04. \tag{3}$$

It does not depend on magnetic field strength *B*. The lifetime of the hypothetical particle confined in the trap behind the barrier can be estimated using the theory of the α-decay [3]. It is supposed that the hypothetical particle has the mass equal to one half of the magnetic mass *M*(*B*) of the magnetoexciton. It performs N_{bl} blows on the back of the barrier trying to escape from the trap and evade tunneling through the barrier. The number of the blows was estimated as follows:

$$N_{bl} \sim \frac{\mathrm{v}_0}{2r_0} \sim \frac{\hbar}{2Mr_0^2} \sim \frac{10^{13}}{\sec}, \tag{4}$$

where r_0 is the radius of the trap.

This number multiplied by the transparency coefficient gives rise to the probability of tunneling

$$P = N_{bl} T \simeq \frac{1}{\tau} \tag{5}$$

and life time τ in the metastable state. It equals to a few picoseconds: $\tau \sim 2.5$ ps. This life time is sufficient to permit the measurement of the radiative recombination process, when one magnetoexciton annihilates with the emission of the cavity photon, if the system is embedded into microcavity, leaving the second exciton in the state of para-magnetoexciton. This process is shown in Fig. 8.

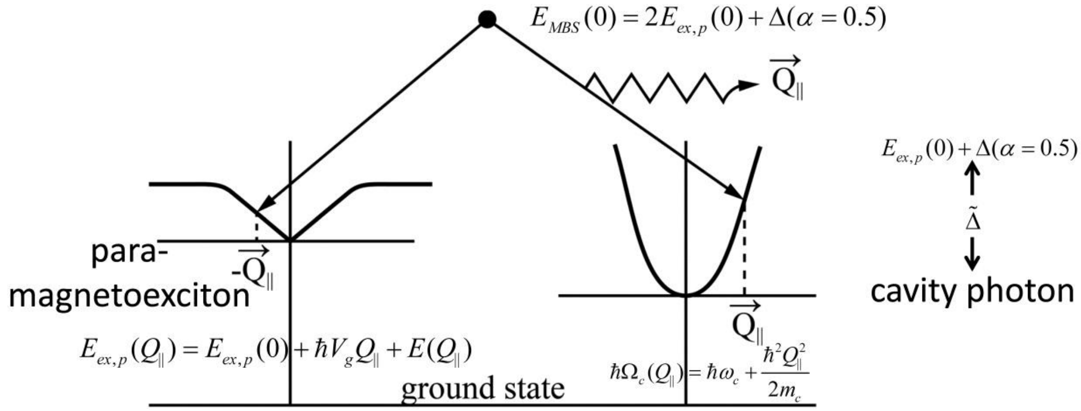

Fig. 8. Radiative recombination of the metastable bound state.

It is the conversion of the metastable state in the para-magnetoexciton. The probability of the conversion was estimated at about $10^8 - 10^{10}\ \mathrm{sec}^{-1}$:

$$P(\omega_c) = \frac{4e^2 m_c |\vec{e}_c \cdot \vec{p}_{c-v}|^2}{\pi c m_0^2 \hbar^2} e^{-\frac{2\tilde{\Delta} m_c l_0^2}{\hbar^2}} \approx 10^8 - 10^{10}\ \frac{1}{\mathrm{sec}}, \tag{6}$$

where

$$m_c = 10^{-5} m_0, \quad l_0 \sim 10^{-6}\ \mathrm{cm}, \ |p_{c-v}| \sim 10^{-20} - 10^{-19}\ \frac{\mathrm{g\ cm}}{\mathrm{sec}}, \ \tilde{\Delta} = E_{ex,p}(0) + \Delta(\alpha = 0.5) - \hbar\omega_c. \tag{7}$$

The probability has a sharp, almost dropping dependence at the high energy side of the band due to the linear dispersion law of the para-magnetoexciton (see Fig. 9).

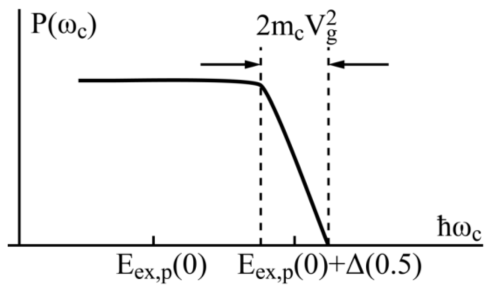

Fig. 9. Probability of the radiative recombination process.

The new luminescence band is shown in Fig. 10. It is located on the high energy side as regards the exciton luminescence line, because the molecular metastable state has the positive energy.

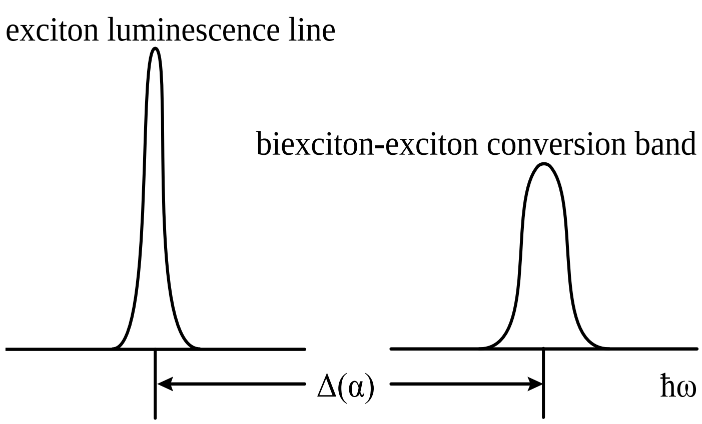

Fig. 10. Luminescence band of the metastable bound state due to radiative recombination with the emission of the photon and with the creation of the para-magnetoexciton. The new luminescence M band is situated at higher frequencies than the frequencies of the para-magnetoexciton luminescence line.

3. Thermodynamics of Para-Magnetoexcitons

To date, it has been known that magnetoexcitons are characterized by the quadratic dispersion law with magnetic mass $M(B)$ increasing with an increase in magnetic field strength B. We have found that the exchange Coulomb e–h interaction, being taken into account supplementary to the direct interaction, leads to the anisotropic linear dispersion law referred to as the anisotropic Dirac cone. It is shown in Fig. 11.

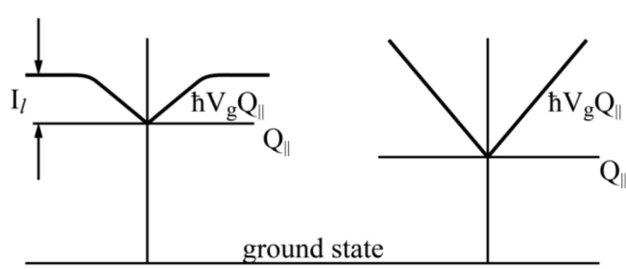

Fig. 11. Anisotropic Dirac cone-like dispersion law of the para-magnetoexciton with linear polarization at the same direction of the wave vector.

The group velocity is present only in the case of para-exciton $(\xi = 1)$ and is absent in the case of ortho-exciton $(\xi = -1)$; it is proportional to oscillator strength f_{ex} of the exciton transition. It means that the anisotropic linear dispersion law appears only in the case of the dipole-active, bright para-magnetoexciton line. The group velocity increases with increasing magnetic field strength:

$$E_{ex,p}(Q_{\|}) = E_{ex,p}(0) + \hbar V_g Q_{\|} + E(Q_{\|}),$$

$$k_B T_c = \left[\frac{2\pi\hbar^2 V_g^2 \sigma}{g_2(1)}\right]^{1/2},$$

$$V_g = \frac{(1+\xi)}{2}\frac{e^2}{\varepsilon_0 \hbar}\left|\frac{\vec{\rho}_{c-v}}{l_0}\right|^2 \sim B; \quad \xi = \begin{cases} +1, \text{ para} \\ -1, \text{ ortho} \end{cases}, \tag{8}$$

where

$$\left|\vec{\rho}_{c-v}\right|^2 \sim f_{ex}\frac{\pi\hbar}{4m_0\omega_{ex}}\left(\frac{a_{ex}}{a_0}\right)^3, \tag{9}$$

and resulted in

$$V_g = \frac{1+\xi}{2} f_{ex}\left(\frac{a_{ex}}{a_0}\right)^3 \frac{\pi e^2}{4m_0\varepsilon_0\omega_{ex}}\frac{1}{l_0^2}, \tag{10}$$

where f_{ex} is the exciton oscillator strength, $\vec{\rho}_{c-v}$ is the inter-band matrix element of the coordinate, ω_{ex} and a_{ex} are the exciton frequency and radius correspondingly, and a_0 is the lattice constant.

The range of the wave vectors, where the linear dispersion takes place is sufficiently large: $k < 1/l_0$. As a consequence, the Bose–Einstein condensation (BEC) conditions for para- and ortho-magnetoexcitons are completely different.

It is well known that the 2D Bose gas with the quadratic dispersion law situated on infinite area S has the BEC temperature equal to zero according to the Hohenberg theorem [4]. To obtain the BEC of cavity exciton polaritons at nonzero temperatures, it was necessary to confine them on the light spot formed by a laser beam on the surface of the quantum well embedded into a microcavity. The experimental physicists' ingenuity succeeded to avoid the Hohenberg theorem.

In the case of the isotropic Dirac cone dispersion law the critical temperature T_c is proportional to group velocity V_g and to the square root of the magnetoexciton density σ. At $V_g = 10^4\ \text{cm/sec}$ and $\sigma = 10^{12}\ \text{cm}^{-2}$, the critical temperature is $1\ \text{K}$. The BEC of para-magnetoexcitons on the state $k = 0$ will be possibly implemented without confining them on the spot.

With the isotropic linear dispersion law, the capacity to accommodate the noncondensed particles in the range of small wave vectors is limited; that is, it is not infinite as was earlier. The BEC of magnetoexcitons on the single-particle state with considerable wave vectors $kl_0 \sim 3-4$ at temperature T=0 was investigated in [5]. In this case, we have the magnetoexcitons with parallel wave vectors and with dipole moments which attract each other. The attraction in the system is an adversary to the BEC. Nevertheless, taking into account the correlation energy and the polarizability of the Bose condensate as a whole using the coherent excited states, it was shown that the metastable Bose–Einstein (BE) condensation at $T=0$ does exist [5]. It is shown in Fig. 12.

Another property of the BEC of magnetoexcitons is the requirement for filling factors ν of the lowest Landau level. They should not exceed the fractional value $1/3\left(\nu \le 1/3\right)$. At this limit, we meet the phenomena encountered in the case of one component 2D electron gas (OC2DEG) under conditions of the fractional quantum Hall effects (FQHEs). As was outlined by Stormer [6], the fascinating properties discovered in the FQHEs arise from the strongly correlated motion of many electrons. It is not fission that leads to fractionally charged quasiparticles, but the interplay of many electrons that “collaborate” and create the bizarre objects (see Fig. 13). For example, the electrons absorb magnetic flux quanta seemingly eliminating the external magnetic field.

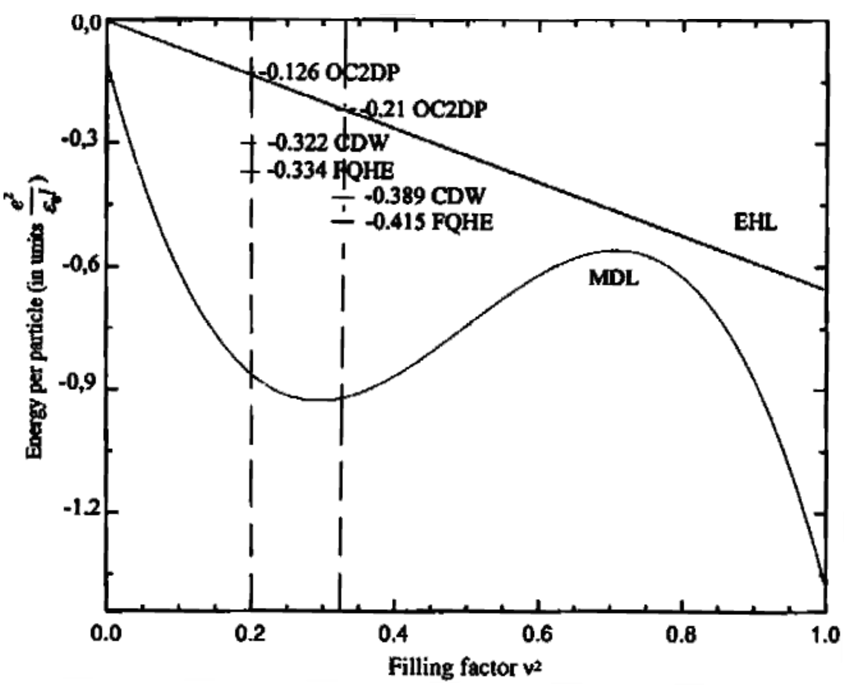

Fig. 12. Energies per particle in units $e^2/(l_0\varepsilon)$ in four different ground states of the OC2DEG and the 2D e–h system, such as: incompressible quantum liquid (IQL) arising under condition of FQHE, charge density wave (CDW), one-component two-dimensional plasma (OC2DP) with the properties similar to those of the e–h liquid (EHL) and the metastable dielectric liquid (MDL) phase formed by BEC 2D magnetoexcitons [5].

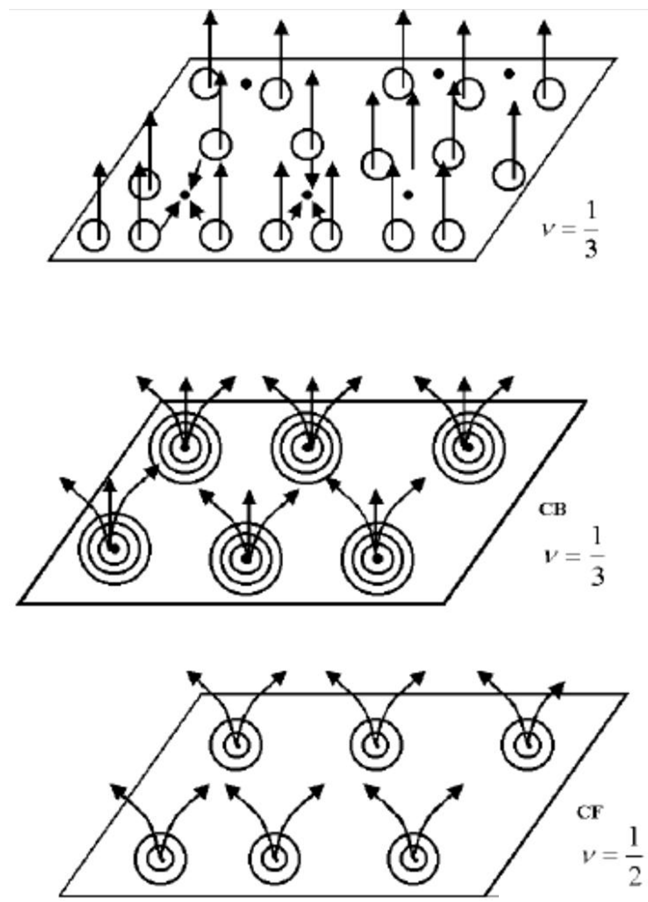

Fig. 13. Vortex content in the composite bosons and composite fermions [6].

Particle statistics are altered from fermionic to bosonic. These properties were revealed studying the 2D electron gas under conditions of the fractional filling factor of the lowest Landau level. When the filling factors of the lowest Landau levels for the electrons and the holes are approaching fractional values, such as $1/2$ and $1/3$, we can expect a similar behavior. The first result in this direction will be communicated. It is well known that new stunning states of the matter were discovered [6–9]. They can be explained using the concept of composite particles arising in the form of electrons with attached flux quanta ϕ_0, as was proposed by Wilczek [7] or, in another version, with attached vortices, as was proposed by Read [8].

The new gauge field created by the quantum point vortices can be introduced into the Hamiltonian by the Chern and Simons unitary transformation $\hat{U}(\vec{r})$, as was proposed by Halperin, Lee, and Read [9].

The flux quanta and the attached vortices to the electrons for filling factor $\nu = 1/2$ and $1/3$ are shown in Fig. 13. It is supposed that each flux quantum generates one quantum point vortex.

Each vortex generates its magnetic field. The flux Φ of the external magnetic field with strength B through the layer surface area S equals to N flux quanta ϕ_0 as follows:

$$\Phi = BS = N\phi_0, \tag{11}$$

where

$$\phi_0 = \frac{2\pi\hbar c}{e} = B\cdot 2\pi l_0, \quad N = \frac{S}{2\pi l_0^2}, \quad l_0^2 = \frac{\hbar c}{eB}. \tag{12}$$

The generated magnetic field compensates the external magnetic field B. It is apparently eliminated and the new composite particles undergo their Fermi degeneracy or their BEC.

Our version with two-component e–h system is shown below. The unitary transformation introducing the Chern–Simons gauge field has the form

$$\hat{U}(\vec{r}) = e^{\frac{ie}{\hbar c}\hat{\omega}(\vec{r})} \tag{13}$$

with vector potential $\vec{a}(\vec{r})$

$$\vec{a}(\vec{r}) = \vec{\nabla}\hat{\omega}(\vec{r}) = -\frac{\phi e}{\alpha}\int d^2\vec{r}\,'\vec{\nabla}\theta(\vec{r}-\vec{r}\,')(\hat{\rho}_e(\vec{r}\,')-\hat{\rho}_h(\vec{r}\,')),$$
$$\phi = 1, 2, 3..., \quad \alpha = e^2/(\hbar c) = 1/137. \tag{14}$$

depending on value $\vec{V}(\vec{r}-\vec{r}\,')$ proportional to the unit azimuthal vector $\vec{\epsilon}_{(\vec{r}-\vec{r}\,')}$ as follows:

$$\vec{V}(\vec{r}-\vec{r}\,') = \frac{\vec{e}_x(\vec{y}-\vec{y}\,')-\vec{e}_y(\vec{x}-\vec{x}\,')}{|\vec{r}-\vec{r}\,'|^2} = \frac{\vec{\epsilon}_{(\vec{r}-\vec{r}\,')}}{|\vec{r}-\vec{r}\,'|}; \qquad \vec{\epsilon}_{(\vec{r}-\vec{r}\,')} = \frac{\vec{e}_x(\vec{y}-\vec{y}\,')-\vec{e}_y(\vec{x}-\vec{x}\,')}{|\vec{r}-\vec{r}\,'|}. \tag{15}$$

The 2D quantum vortex has the center at point $\vec{r}$ and the velocity at point $\vec{r}\,'$, as shown in Fig. 14 with the property

$$\mathrm{curl}\,\vec{V}(\vec{r}-\vec{r}\,') = \Delta\ln|\vec{r}-\vec{r}\,'| = 2\pi\delta^2(\vec{r}-\vec{r}\,'). \tag{16}$$

The bare and the dressed field operators are

$$\hat{\psi}_e(\vec{r}) = \hat{U}^+(\vec{r})\hat{\psi}_e^0(\vec{r}); \quad \hat{\psi}_h(\vec{r}) = \hat{U}(\vec{r})\hat{\psi}_h^0(\vec{r}). \tag{17}$$

The bare electron and hole operators obey the Fermi statistics:

$$\hat{\psi}_i^0(\vec{r})\hat{\psi}_j^{0\dagger}(\vec{r}\,')+\hat{\psi}_j^{0\dagger}(\vec{r}\,')\hat{\psi}_i^0(\vec{r}) = \delta_{ij}\delta^2(\vec{r}-\vec{r}\,'), \tag{18}$$

whereas the composite particles are described by new operators (17). They obey Fermi or Bose statics depending on the even or odd numbers, respectively, of parameter ϕ in definition (14).

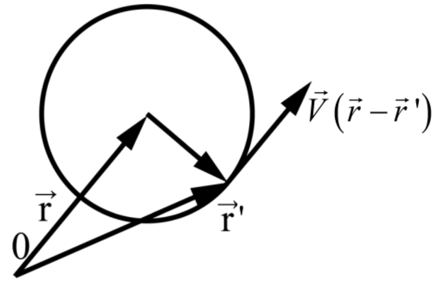

Fig. 14. 2D quantum point vortex with the velocity at point $\vec{r}\,'$ and singular vorticity at point $\vec{r}$.

In our case, vector potential $\vec{a}(\vec{r})$ of the Chern–Simons field depend on the difference between the densities of the electrons and the holes, $\hat{\rho}_e(\vec{r}\,')$ and $\hat{\rho}_h(\vec{r}\,')$. In the zeroth approximation, when the density operators can be substituted by their average values, the new vector potential vanishes. The external magnetic field does not disappear. It continues to effectuate the Landau quantization of the composite particles.

The statistics of the composite particles is changed simultaneously for the electrons and the holes because they attach an equal number of vortices. Kinetic energies of the composite particles look as follows:

$$\frac{\hbar^2}{2m_e}\left(-i\vec{\nabla}_e+\frac{e}{\hbar c}\vec{A}(\vec{r}_e)+\frac{e}{\hbar c}\hat{\vec{a}}(\vec{r}_e)\right)^2+\frac{\hbar^2}{2m_h}\left(-i\vec{\nabla}_h-\frac{e}{\hbar c}\vec{A}(\vec{r}_h)-\frac{e}{\hbar c}\hat{\vec{a}}(\vec{r}_h)\right)^2. \tag{19}$$

The Coulomb interaction gives rise to the binding energy, the ionization potential, and the dispersion law (Fig. 15) due to the strong interdependence between the center-of-mass and the relative e–h motions.

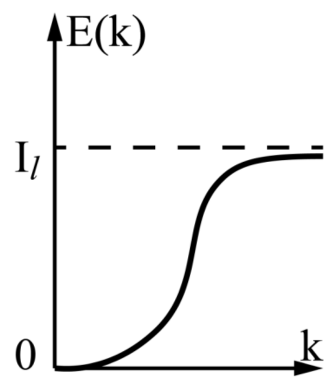

Fig. 15. Dispersion law of the magnetoexciton.

In the first order of the perturbation theory, one can observe how the new gauge field affects the magnetoexcitons currently consisting of composite electrons and holes. It was shown that, in addition to the previous isotropic term of the dispersion law shown above in Fig. 15, new anisotropic components of the magnetic mass appear. The isotropic magnetic mass $M(B)$ due to the Coulomb interaction and anisotropic components M_x and M_y due to new gauge vector potential are as follows:

$$M(B) = \frac{\hbar^2}{2I_l l_0^2} = \frac{\hbar^2 \varepsilon_0}{\sqrt{2\pi} e^2 l_0},$$

$$\left(\frac{1}{m_e} - \frac{1}{m_h}\right) M_x = \frac{2\alpha \hbar^2 c^2}{3\phi e^3 l_0^2 B} \approx 0.4; \quad M_y = 3M_x, \tag{20}$$

where $l_0 = 10^{-6}\ \mathrm{cm}^2$ at a magnetic field strength of B = 6 T. It takes place when effective masses m_e and m_h do not coincide. The isotropic mass increases with increasing magnetic field strength B, whereas the anisotropic component does not depend on it.

4. Conclusions

In the lowest Landau levels approximation, stable bound states of the magnetic biexcitons do not exist due to the hidden symmetry in the e–h system.

The metastable bound state with a lifetime of about few picoseconds has been revealed.

The conversion of the metastable bound state into the para-magnetoexciton state gives rise to a new luminescence band situated at higher frequencies than those of the para-magnetoexciton luminescence line.

The allowance for the exchange e–h Coulomb interaction in the case of the dipole-active para-magnetoexcitons leads to the dispersion law of the anisotropic Dirac cone-type.

The isotropic Dirac cone-type dispersion law gives rise to the finite temperature of the BEC of the 2D magnetoexciton gas.

The Chern–Simons gauge field leads to the formation of composite electrons and holes with equal numbers of attached quantum point vortices.

The effective magnetic field created by quantum point vortices in the case of the coplanar 2D e–h system vanishes in the mean-field approximation, and the composite particles undergo the Landau quantization as a whole in an external magnetic field.

The vector potentials of the external magnetic field and of the gauge Chern–Simons field lead to the anisotropy of the 2D magnetoexciton magnetic mass.

References

[1] D. Paquet, T. M. Rice, and K. Ueda, Phys. Rev. B 32, 5208 (1985).
[2] I. V. Lerner and Yu. E. Lozovik, Zh. Eksp. Teor. Fiz. 80, 1488 (1981) [Sov. Phys. – JETP 53, 763 (1981)].
[3] D. I. Blokhintsev, Quantum Mechanics, D. Reidel Publishing Company, Dordrecht, Holland, Springer Netherlands, 1964.
[4] P. C. Hohenberg, Phys. Rev. 158, 3837 (1967).
[5] S. A. Moskalenko, M. A. Liberman, D. W. Snoke, and V. Botan, Phys. Rev. B 66, 245316 (2002).
[6] H. L. Stormer, Rev. Mod. Phys. 71, 4, 875 (1999).
[7] F. Wilczek, Phys. Rev. Lett. 48, 1144 (1982); 49, 957 (1982).
[8] N. Read, Phys. Rev. B 58, 16262 (1998).
[9] B. I. Halperin, P. A. Lee, and N. Read, Phys. Rev. B 47, 7312 (1993).